Published in final edited form as:

AJR Am J Roentgenol. 2020 December ; 215(6): 1436–1442. doi:10.2214/AJR.19.22187.

Ferumoxytol-Enhanced MRI Is Not Inferior to Gadolinium-Enhanced MRI in Detecting Intracranial Metastatic Disease and Metastasis Size

Bronwyn E. Hamilton[1], **Ramon Barajas**[1], **Gary M. Nesbit**[2], **Rongwei Fu**[3], **Prakash Ambady**[4], **Matthew Taylor**[5], **Edward A. Neuwelt**[4,6]

[1]Department of Radiology, Oregon Health & Science University, Portland, [2]Department of Neurointerventional Surgery, Oregon Health & Science University, Portland, [3]School of Public Health, Oregon Health & Science University, Portland, [4]Department of Neuro-Oncology, Oregon Health & Science University, Portland, [5]Department of Hematology-Oncology, Oregon Health & Science University, Portland, [6]Department of Neurology, Oregon Health & Science University, 3181 SW Sam Jackson Park Rd, Portland,

Abstract

OBJECTIVE.—The goal of this intraindividual comparison study was to investigate whether ferumoxytol-enhanced MRI is as effective as standard-of-care gadolinium-enhanced MRI in detecting intracranial metastatic disease.

MATERIALS AND METHODS.—We retrospectively reviewed all patients who underwent imaging as part of two ongoing ferumoxytol-enhanced and gadolinium-enhanced MRI protocol studies to compare the number and size of enhancing metastatic lesions. Two neuroradiologists independently measured enhancing metastases on ferumoxytol-enhanced MR images and on control gadolinium-enhanced MR images. The number and size of metastases were compared on an intraindividual basis. Primary diagnoses were recorded. A linear mixed-effects model was used to compare differences in cubic root of volume between gadolinium-enhanced and ferumoxytol-enhanced MRI. A signed rank test was used to evaluate differences between reviewers.

RESULTS.—MR images from 19 patients with brain metastases were analyzed (seven with lung cancer, three with breast cancer, three with melanoma, two with ovarian cancer, one with colon cancer, one with renal cell carcinoma, one with carcinoid tumor, and one with uterine cancer). Reviewer 1 identified 77 masses on ferumoxytol-enhanced MRI and 72 masses on gadolinium-enhanced MRI. Reviewer 2 identified 83 masses on ferumoxytol-enhanced MRI and 78 masses on gadolinium-enhanced MRI. For reviewer 1, ferumoxytol-enhanced MRI showed a mean tumor size measuring 1.1 mm larger in each plane compared with gadolinium-enhanced MRI (p = 0.1887). For reviewer 2, ferumoxytol-enhanced MRI showed a mean tumor size measuring 1.0 mm larger in each plane (p = 0.2892). No significant differences in number of metastases or tumor sizes were observed between contrast agents or reviewers.

Address correspondence to E. A. Neuwelt (neuwelte@ohsu.edu).

CONCLUSION.—Intracranial metastatic disease detection with ferumoxytol-enhanced MRI was not inferior to detection with gadolinium-enhanced MRI. Ferumoxytol-enhanced MRI could improve workup and monitoring of patients with brain metastases if gadolinium-enhanced MRI is contraindicated.

Keywords

brain metastases; contrast agents; ferumoxytol

Gadolinium-based contrast agents (GBCAs) are critical for MRI evaluation of intracranial masses. GBCA-enhanced MRI is the reference standard for image depiction of brain metastases.

GBCAs have been safely administered more than 300 million times [1, 2] with a very low frequency of acute adverse events. However, several well-established clinical scenarios have emerged in which a small number of patients have contraindications to GBCA administration, including diminished renal function and severe prior allergic reaction [3–5]. Patients who are unable to safely receive GBCAs require an alternative method of detecting brain metastases for proper treatment and surveillance. Enhanced CT is inferior to gadolinium-enhanced MRI and can easily miss small brain metastases.

Ferumoxytol (Feraheme, Amag Pharmaceuticals) is a unique ultrasmall superparamagnetic iron oxide nanoparticle that has been successfully used as a molecular MRI contrast agent to localize the intravascular and neurovascular unit compartments of the blood-brain barrier. Although ferumoxytol has not been approved by the Food and Drug Administration (FDA) as an imaging contrast agent, off-label use of the agent has shown benefit in patients with contraindications to gadolinium-enhanced MRI.

Thus, ferumoxytol-enhanced MRI could also offer an alternative to patients without metastatic disease given the growing concern about gadolinium deposits in the brain in patients who have previously undergone gadolinium-enhanced MRI [6, 7]. Although no adverse clinical outcomes have been linked with cerebral GBCA deposition, many multinational regulatory agencies continue to investigate the long-term health risks of gadolinium deposition in the brain.

The objective of our study was to assess whether a difference in brain metastasis detection rate exists between anatomic ferumoxytol-enhanced MRI (case group) and standard-of-care anatomic gadolinium-enhanced MRI (control group). We hypothesized that T1 shortening, which occurs with accumulation of ultrasmall superparamagnetic iron oxide within CNS metastatic foci, using ferumoxytol-enhanced MRI is not inferior to T1 shortening using gadolinium-enhanced MRI and allows similar lesion detection rates. Furthermore, we hypothesized that T2 shortening is superior to GBCA use. To test these hypotheses, two neuroradiologists independently compared metastasis detection rate and size on T1- and T2-weighted ferumoxytol-enhanced and gadolinium-enhanced MR images.

Materials and Methods

For this retrospective unblinded intraindividual comparison study, patients were selected from one of two ongoing prospective ferumoxytol-enhanced and gadolinium-enhanced MRI studies (protocol 813 and protocol 1562), which were approved by our institutional review board for evaluating the value of ferumoxytol-enhanced MRI in detecting CNS malignancy and inflammatory and vascular disease. Given the retrospective nature of the design, no randomization for crossover was feasible. Inclusion criteria required a diagnosis of disease that had metastasized to the brain and available ferumoxytol-enhanced MR images for review. The primary cancer diagnosis was confirmed pathologically in all patients, whereas brain metastatic involvement was confirmed pathologically in patients for whom surgical resection was indicated. For those with contraindications or considerations precluding brain biopsy or resection, diagnosis of brain metastases was based on the primary cancer diagnosis in addition to histopathologic confirmation of metastatic disease. For patients who did not undergo surgical confirmation of brain metastases, typical MRI findings consistent with brain metastases with or without tissue confirmation of metastatic disease elsewhere were used.

Patients included in these study protocols underwent gadolinium-enhanced MRI as part of their imaging study within 1 or 2 days before ferumoxytol-enhanced MRI if contemporaneous clinical gadolinium-enhanced MRI was not available. Of the patients included in either study who had recently undergone clinical gadolinium-enhanced MRI but for whom the requirement to undergo on-protocol gadolinium-enhanced MRI within 1 day before ferumoxytol-enhanced MRI was waived, we included those with a clinical or off-study-protocol gadolinium-enhanced MRI study available for comparison, provided it was obtained within 30 days before the ferumoxytol-enhanced MRI study (to minimize the potential for change in metastasis size, number, or visibility due to growth or response during the allowed time interval). However, patients who underwent clinical gadolinium-enhanced MRI within 5 days after the ferumoxytol-enhanced MRI study were excluded given that residual enhancement can last several days after ferumoxytol injection. Because of this limitation, gadolinium-enhanced MRI was always performed before ferumoxytol-enhanced MRI according to study protocol.

All patients who underwent on-protocol gadolinium-enhanced MRI received a single weight-appropriate dose (0.1 mmol/kg) of gadoteridol (ProHance, Bracco). For off-protocol gadolinium-enhanced MRI, the specific contrast agent was not routinely available. All MRI examinations that were part of the research protocol (gadolinium-enhanced and ferumoxytol-enhanced MRI) were performed on one of two 3-T systems (Achieva, Philips Healthcare) using an eight-channel sensitivity-encoding transmit-receive coil. For patients who underwent off-protocol imaging, this information was not always available.

Injection rates for ferumoxytol-enhanced MRI varied because of dynamic susceptibility contrast and steady-state perfusion imaging requirements for a different study; these perfusion data were not analyzed for the present study. Injection rates were lowered after a black box warning for ferumoxytol was issued by the FDA in 2015.

Total dose infusion time was usually 10 minutes or more after adjustment. Only the anatomic contrast-enhanced series of images (not the perfusion imaging) were reviewed for the purposes of this study. Sequence parameters are delineated in Table 1 for protocol 813 and Table 2 for protocol 1562.

On the basis of our prior published data, we have found that anatomic enhancement with ferumoxytol in MRI of brain tumors is optimized with a longer delay of approximately 24 hours before imaging as compared with gadolinium enhancement. Thus, a baseline unenhanced MR image is obtained on day 1 and is followed by IV ferumoxytol injection. Performing MRI on day 2 allows the imaging sequences to be repeated (without any further IV injection of ferumoxytol) for evaluation of anatomic enhancement. Thus, the ferumoxytol-enhanced MR images were compared with the unenhanced baseline images obtained on day 1 and were used to measure enhancing tumor size in this study. The study design allowed ferumoxytol-enhanced MRI to be performed either 1 or 2 days after gadolinium-enhanced MRI according to protocol.

Two faculty neuroradiologists (one with 18 years of experience and one with no prior experience interpreting iron oxide nanoparticle–enhanced MRI) independently measured enhancing metastatic foci on ferumoxytol-enhanced MR images. The reviewer without experience interpreting ferumoxytol-enhanced MR images was informed about the different mechanism of enhancement with ferumoxytol compared with gadolinium and, in particular, the need to review contrast-enhanced T2-weighted images for new hypoenhancement. We used reviewers with different levels of experience in part to show that no difference in measurement ability existed between reviewers, suggesting that formal training is not required to interpret ferumoxytol-enhanced MRI. The same radiologists performed a second review of the gadolinium-enhanced MR images, although no specific time interval between the reviews was set. Size of metastasis (rounded to the nearest tenth of a millimeter in three orthogonal planes), location in the brain, total number of metastases, and specific tumor diagnosis based on histopathology were recorded for all patients according to both ferumoxytol-enhanced and gadolinium-enhanced MRI. All discrepant findings underwent consensus review to assess why lesions were missed by use of either technique.

Ferumoxytol may cause T2 shortening in addition to typical enhancement related to T1 shortening, so T2-weighted sequences were also evaluated qualitatively for new hypointense lesions on ferumoxytol-enhanced MRI compared with unenhanced T2-weighted imaging. Because this might result in interpretive errors by radiologists unfamiliar with ferumoxytol-enhanced MRI, we assessed the frequency of this finding.

A linear mixed-effects model was used to compare the differences in the cubic root of volume between gadolinium-enhanced and ferumoxytol-enhanced MRI based on linear three-plane measurements and also accounted for multiple lesions within a patient. The three-plane difference in volume was not evaluated because absolute differences were highly related to tumor size with variations in morphologic features, and because this was not considered the best measure for evaluating differences between gadolinium-enhanced and ferumoxytol-enhanced MRI. Distribution of the cubic root of volume was used instead,

which satisfied the assumption of a normal distribution and provided a better measure for comparing ferumoxytol-enhanced and gadolinium-enhanced MRI.

The signed rank test (nonparametric test because of nonnormal distribution) was used to assess differences between reviewers, with a $p < 0.05$ considered significant.

Results

A total of 27 patients were identified from imaging protocols 813 and 1562. Five patients were excluded because they did not undergo ferumoxytol-enhanced MRI 24 hours after the baseline MRI examination, two were excluded because they did not undergo gadolinium-enhanced MRI within 30 days before undergoing ferumoxytol-enhanced MRI, and one was excluded because no intracranial metastasis was found (an enhancing temporal lobe mass was diagnosed as radionecrosis on the basis of pathologic confirmation). After these exclusions, 19 patients remained for analysis. Of these remaining 19 subjects, nine did not undergo gadolinium-enhanced MRI according to protocol, so clinical gadolinium-enhanced MRI was substituted instead.

The distribution of primary malignancies included lung cancer in seven patients (six with non–small cell and one with small cell carcinoma), breast cancer in three, melanoma in three, ovarian cancer in two, renal cell carcinoma in one, carcinoid tumor in one, colon adenocarcinoma in one, and uterine sarcoma in one. Brain metastases were confirmed pathologically in 12 of 19 patients, whereas the remaining brain metastases were diagnosed based on patients' known primary cancer, observation of typical imaging, presence of additional distant metastatic disease elsewhere, or a combination of these methods.

Reviewer 1 identified 77 masses on ferumoxytol-enhanced MRI and 72 masses on gadolinium-enhanced MRI. Reviewer 2 identified 83 masses on ferumoxytol-enhanced MRI and 78 masses on gadolinium-enhanced MRI (Table 3). No significant differences were observed between reviewers with respect to either the number of metastases or tumor volume for either ferumoxytol-enhanced or gadolinium-enhanced MRI (Figs. 1–3). All patients with metastatic disease on gadolinium-enhanced MRI also had metastatic disease on ferumoxytol-enhanced MRI. A discordant number of enhancing metastases were seen on gadolinium-enhanced compared to ferumoxytol-enhanced MRI in 14 of 19 patients for both reviewers. Reviewer 1 observed 54 new hypointense lesions on ferumoxytol-enhanced MRI, and reviewer 2 observed 57.

The reviewers found slightly different numbers of metastatic foci in five patients with multiple lesions, although the differences were not significant. Consensus review of these discrepancies showed concordance for all lesions in four of the five patients. Missed foci appeared to be due to small or punctate metastasis or conspicuity, potentially attributed to reader fatigue. For the fifth patient, concordance was also achieved on consensus review (25 masses on ferumoxytol-enhanced MRI and 18 on gadolinium-enhanced MRI), with discrepancies likely due to reader fatigue and indeterminate punctate enhancing foci. In this case, the difference in the number of metastases detected on consensus review was likely due to technique differences (thin-slice 3D ferumoxytol-enhanced MRI compared with

standard-slice 2D gadolinium-enhanced MRI), lesion growth in the 20-day interval between clinical gadolinium-enhanced MRI (performed first) and ferumoxytol-enhanced MRI (performed second), or both.

For reviewer 1, ferumoxytol-enhanced MRI showed a mean tumor size measuring 1.1 mm larger on average in each plane compared with gadolinium-enhanced MRI ($p = 0.1887$). Translating to relative difference, ferumoxytol-enhanced MRI showed a mean increase in tumor of 20% on average in each plane compared with gadolinium-enhanced MRI or a 73% increase in median volume ($1.2^3 = 1.73$) compared with the median volume for gadolinium-enhanced MRI

For reviewer 2, ferumoxytol-enhanced MRI showed a mean tumor size measuring 1.0 mm larger on average in each plane compared with gadolinium-enhanced MRI ($p = 0.2892$). Translating to relative difference, ferumoxytol-enhanced MRI showed a mean increase in tumor of 18% on average in each plane compared with gadolinium-enhanced MRI or a 64% increase in median volume ($1.18^3 = 1.64$) compared with the median volume for gadolinium-enhanced MRI.

The median difference in number of metastatic foci detected between reviewers was 0 for both gadolinium-enhanced and ferumoxytol-enhanced MRI (reflecting no significant difference, $p = 0.1250$). The median difference in total cubic root of volume on gadolinium-enhanced MRI was −301.6, with no significant difference between reviewers ($p = 0.6095$). The median difference in total cubic root of volume on ferumoxytol-enhanced MRI was 524, with no significant difference between reviewers ($p = 0.2101$).

Discussion

The current study compared the use of ferumoxytol-enhanced MRI with the standard-of-care control, gadolinium-enhanced MRI, for the detection of intracranial metastatic foci. Our findings provide evidence that ferumoxytol-enhanced MRI is not inferior to gadolinium-enhanced MRI for detecting intracranial metastatic foci and suggest that ferumoxytol-enhanced MRI is clinically useful in patients unable to undergo gadolinium-enhanced MRI.

Patients who are unable to safely receive GBCAs because of either allergies or contraindications could benefit from ferumoxytol-enhanced MRI because no other effective imaging option exists for detecting brain metastases. This is particularly true for patients with renal failure and estimated glomerular filtration rates less than 30 mL/min, who are at risk for nephrogenic systemic fibrosis. Enhanced CT might be an option for some of these patients but is far less sensitive than enhanced MRI.

Many patients and referring physicians are reluctant to use GBCAs because of potential retention in the brain in addition to impaired renal function or contrast agent allergy. This is a greater concern in patients undergoing high-frequency brain MRI screening, such as those with later-stage melanoma. The possibility of retention has even led to reevaluation of the need for contrast agents in MRI of metastatic disease, with results of one study confirming that enhanced T1-weighted MRI is the best detection method [8].

Interpretation of ferumoxytol-enhanced MRI is relatively straightforward and similar to interpretation of gadolinium-enhanced MRI. Differing levels of experience in interpreting ferumoxytol-enhanced MRI did not appear to affect the results, because no significant difference was observed between reviewers regarding the number or size of metastatic lesions. Taking all metastatic lesions into consideration, both reviewers identified more total lesions on ferumoxytol-enhanced MRI than on gadolinium-enhanced MRI, though this difference was not significant. Retrospective consensus review found that all metastases on gadolinium-enhanced MRI were seen on ferumoxytol-enhanced MRI and that one patient had more lesions on ferumoxytol-enhanced MRI than on gadolinium-enhanced MRI. Analysis showed that the discrepancy in this latter patient was attributed to technique difference and time delay between the two scans.

A trend toward larger tumor volume on ferumoxytol-enhanced MRI was suggested but could not be confirmed statistically because of insufficient power and the wide variation in size of individual masses. However, a number of explanations are possible. First, tumor growth could have occurred during the delay between clinical gadolinium-enhanced MRI and ferumoxytol-enhanced MRI, which was performed many days later. Additional factors include the technical variations (sequence type, slice thickness, field strength, and specific GBCA or dose) that are inherent when including patients who have undergone uncontrolled clinical gadolinium-enhanced MRI.

Ferumoxytol-enhanced MR images may depict intrinsically larger lesion sizes than gadolinium-enhanced MR images because of perilesional macrophage uptake (a primary mechanism of enhancement with ferumoxytol) that may enhance outside of the actual metastasis. Susceptibility effects are also possible but overall not likely for standard spin-echo T1 and T2 imaging. Because most ferumoxytol-enhanced MRI studies were performed within 24 hours after gadolinium-enhanced MRI (and after a longer interval in a few cases), interval growth, although possible, seems unlikely.

Prior studies have shown larger areas of enhancement in some lesions with iron oxide nanoparticles in CNS pathologic diseases, which was thought to be due to inflammatory cellular uptake [8, 9]. CNS metastases may have sufficiently large blood-brain barrier leakage that could allow two mechanisms of enhancement: macrophage uptake and blood-brain barrier disruption. We have anecdotal evidence of some metastases enhancing immediately after IV ferumoxytol injection, although that enhancement was more intense or larger than that seen on subsequent imaging. Prior studies confirmed localization of a precursor iron oxide contrast agent, ferumoxtran-10, in phagocytic white cells, and primary CNS gliomas showed a similar pattern of larger size on ferumoxytol-enhanced MRI compared with gadolinium-enhanced MRI [8, 9].

Ferumoxytol-enhanced MRI could also prove useful in evaluating treatment-related inflammation or pseudoprogression in metastatic disease. Our experience with perfusion-based ferumoxytol-enhanced MRI has shown value in distinguishing pseudoprogression and true progression in primary CNS malignancies [10, 11]. Pseudoprogression also occurs in metastatic disease [12, 13]. Posttreatment MRI evaluation of intracranial metastases is similarly limited by the inability of anatomic imaging to distinguish between active disease

and pseudoprogression, particularly given newer immunotherapies [14]. Other techniques used to better assess this complication include gadolinium-based dynamic susceptibility contrast perfusion-weighted imaging and delayed contrast extravasation [15–17], though none are sufficiently predictive.

Our work with ferumoxytol-based dynamic susceptibility contrast perfusion-weighted imaging and steady-state perfusion imaging [9, 11] to differentiate pseudoprogression from true progression might offer similar value in metastatic disease. Ferumoxytol-based perfusion MRI is reproducible and, unlike GBCA-based perfusion-weighted imaging, requires no postprocessing leakage correction or dose preloading. These advantages could confer benefit in clinical trials by allowing accurate diagnosis and reproducibility across institutions, which is not currently feasible.

The current barrier to clinical use is the lack of FDA labeling. In 2015, the FDA relabeled ferumoxytol with a black box warning because of a risk of anaphylactoid reactions that was higher than initially detected [18]. This action was based on surveillance safety data from ferumoxytol use for its labeled indication of IV iron replacement in patients with renal failure; rapid IV bolus doses were given as two 510-mg IV injections over 17 seconds, each at a rate of 1 mL (30 mg of iron) per second [19]. Because of these data and the FDA's black box warning, we modified our imaging protocols to use slower infusion rates.

According to our own institutional experience [20] and the FeraSafe multicenter MRI registry [21], which includes 4240 ferumoxytol injections for MRI purposes from 11 partner institutions at nine U.S. academic medical centers and two academic medical centers in the United Kingdom, no severe (grade 4 or 5) allergic reactions have been reported with ferumoxytol when lower infusion rates are used for MRI.

The limitations of our study include its small sample size and use of clinical gadolinium-enhanced MRI studies. Minor differences in tumor detection and tumor size on clinical gadolinium-enhanced MRI compared with ferumoxytol-enhanced MRI likely led to minor differences in the detection rate because of timing or differences in MRI technique. This was unavoidable for two reasons. First, ferumoxytol-enhanced MRI cannot be performed shortly before gadolinium-enhanced MRI because of the possibility of retained contrast medium that can persist many days after ferumoxytol injection (precluding accurate assessment of enhancement if GBCAs are administered during this time frame). Second, these data were obtained retrospectively using clinical gadolinium-enhanced MRI performed earlier in a subset of patients. The observation that T2 hypointensity occurs only with ferumoxytol-enhanced MRI suggests that ferumoxytol might improve metastasis detection; however, the most important aspect of this finding is radiologist awareness, which helps to avoid misdiagnosis of metastases as hemorrhage.

Conclusion

In this retrospective study, ferumoxytol-enhanced MRI was not inferior to gadolinium-enhanced MRI for detecting intracranial metastatic disease and lesion size. Ferumoxytol-

enhanced MRI could be useful in the workup and monitoring of patients with metastatic brain disease if gadolinium-enhanced MRI is contraindicated.

Acknowledgments

We thank Heather Leon and Lisa Muir for their assistance with this article.

Ferumoxytol ultrasmall superparamagnetic iron oxide nanoparticles were partially donated by Amag Pharmaceuticals. Oregon Health & Science University received a sponsored research agreement from Amag Pharmaceuticals to conduct clinical trials of MRI with ferumoxytol. None of the authors has financial interest in this agent or in its developer, Amag Pharmaceuticals.

Supported in part by grants CA199111, CA137488, and CA137488-15S1 from the National Institutes of Health; grant BX003897 from the Veterans Affairs Merit Review program; and the Walter S. and Lucienne Driskill Foundation (all support to E. A. Neuwelt).

References

1. Runge VM. Macrocyclic versus linear gadolinium chelates. Invest Radiol 2015; 50:811 [PubMed: 26523911]
2. Reeder SB, Gulani V. Gadolinium deposition in the brain: do we know enough to change practice? Radiology 2016; 279:323–326
3. Li A, Wong CS, Wong MK, Lee CM, Au Yeung MC. Acute adverse reactions to magnetic resonance contrast media: gadolinium chelates. Br J Radiol 2006; 79:368–371 [PubMed: 16632615]
4. Thomsen HS. Contrast media safety—an update. Eur J Radiol 2011; 80:77–82 [PubMed: 21856102]
5. Kribben A, Witzke O, Hillen U, Barkhausen J, Daul AE, Erbel R. Nephrogenic systemic fibrosis: pathogenesis, diagnosis, and therapy. J Am Coll Cardiol 2009; 53:1621–1628 [PubMed: 19406336]
6. Semelka RC, Ramalho M, AlObaidy M, Ramalho J. Gadolinium in humans: a family of disorders. AJR 2016; 207:229–233 [PubMed: 27224028]
7. McDonald RJ, McDonald JS, Kallmes DF, et al. Intracranial gadolinium deposition after contrast-enhanced MR imaging. Radiology 2015; 275:772–782 [PubMed: 25742194]
8. Manninger SP, Muldoon LL, Nesbit G, Murillo T, Jacobs PM, Neuwelt EA. An exploratory study of ferumoxtran-10 nanoparticles as a blood-brain barrier imaging agent targeting phagocytic cells in CNS inflammatory lesions. AJNR 2005; 26:2290–2300 [PubMed: 16219835]
9. Varallyay P, Nesbit G, Muldoon LL, et al. Comparison of two superparamagnetic viral-sized iron oxide particles ferumoxides and ferumoxtran-10 with a gadolinium chelate in imaging intracranial tumors. AJNR 2002; 23:510–519 [PubMed: 11950637]
10. Deike-Hofmann K, Thünemann D, Breckwoldt MO, et al. Sensitivity of different MRI sequences in the early detection of melanoma brain metastases. PLoS One 2018; 13:e0193946 [PubMed: 29596475]
11. Gahramanov S, Muldoon LL, Varallyay CG, et al. Pseudoprogression of glioblastoma after chemo- and radiation therapy: diagnosis by using dynamic susceptibility-weighted contrast-enhanced perfusion MR imaging with ferumoxytol versus gadoteridol and correlation with survival. Radiology 2013; 266:842–852 [PubMed: 23204544]
12. Varallyay CG, Nesbit E, Fu R, et al. High-resolution steady-state cerebral blood volume maps in patients with central nervous system neoplasms using ferumoxytol, a superparamagnetic iron oxide nanoparticle. J Cereb Blood Flow Metab 2013; 33:780–786 [PubMed: 23486297]
13. Lawrence YR, Li XA, el Naqa I, et al. Radiation dose-volume effects in the brain. Int J Radiat Oncol Biol Phys 2010; 76(suppl):S20–S27 [PubMed: 20171513]
14. Parvez K, Parvez A, Zadeh G. The diagnosis and treatment of pseudoprogression, radiation necrosis and brain tumor recurrence. Int J Mol Sci 2014; 15:11832–11846 [PubMed: 24995696]
15. de Velasco G, Krajewski KM, Albiges L, et al. Radiologic heterogeneity in responses to anti-PD-1/PD-L1 therapy in metastatic renal cell carcinoma. Cancer Immunol Res 2016; 4:12–17 [PubMed: 26589768]

16. Choi YJ, Kim HS, Jahng GH, Kim SJ, Suh DC. Pseudoprogression in patients with glioblastoma: added value of arterial spin labeling to dynamic susceptibility contrast perfusion MR imaging. Acta Radiol 2013; 54:448–454 [PubMed: 23592805]

17. Zach L, Guez D, Last D, et al. Delayed contrast extravasation MRI: a new paradigm in neuro-oncology. Neuro Oncol 2015; 17:457–465 [PubMed: 25452395]

18. Food and Drug Administration website. FDA drug safety communication: FDA strengthens warnings and changes prescribing instructions to decrease the risk of serious allergic reactions with anemia drug Feraheme (ferumoxytol). www.fda.gov/drugs/drug-safety-and-availability/fda-drug-safety-communication-fda-strengthens-warnings-and-changes-prescribing-instructions-decrease. Published March 30, 2015. Accessed August 20, 2019

19. Provenzano R, Schiller B, Rao M, Coyne D, Brenner L, Pereira BJ. Ferumoxytol as an intravenous iron replacement therapy in hemodialysis patients. Clin J Am Soc Nephrol 2009; 4:386–393 [PubMed: 19176796]

20. Varallyay CG, Toth GB, Fu R, et al. What does the boxed warning tell us? Safe practice of using ferumoxytol as an MRI contrast agent. AJNR 2017; 38:1297–1302 [PubMed: 28495944]

21. Nguyen KL, Yoshida T, Kathuria-Prakash N, et al. Multicenter safety and practice for off-label diagnostic use of ferumoxytol in MRI. Radiology 2019; 293:554–564 [PubMed: 31638489]

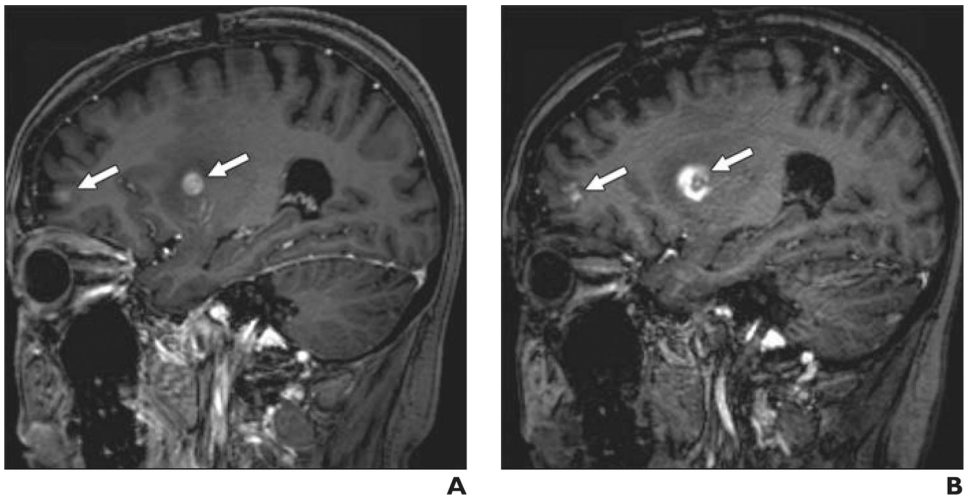

Fig. 1—.

48-year-old woman with breast cancer metastatic to brain.

A, Sagittal 3D T1-weighted magnetization-prepared rapid acquisition gradient echo gadolinium-enhanced MR image, obtained according to protocol, shows multiple brain metastases (*arrows*).

B, Sagittal 3D T1-weighted magnetization-prepared rapid acquisition gradient echo ferumoxytol-enhanced MR image acquired 1 day after image in **A** shows multiple brain metastases (*arrows*). Larger size of right basal ganglia lesion may be due to perilesional macrophages or inflammation.

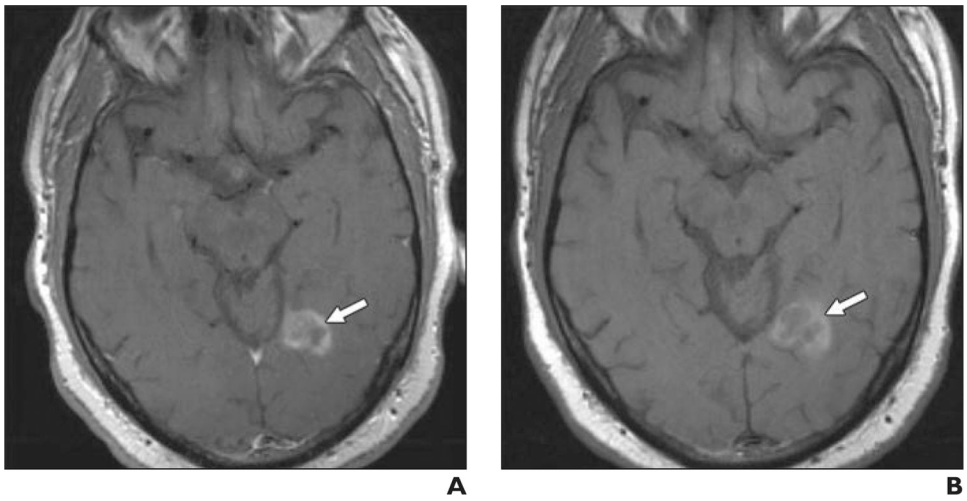

Fig. 2—.

53-year-old man with lung cancer metastatic to brain.

A, Axial T1-weighted turbo spin-echo gadolinium-enhanced MR image, obtained according to protocol, shows left occipital metastasis (*arrow*).

B, Axial T1-weighted turbo spin-echo ferumoxytol-enhanced MR image obtained 1 day after image in **A** shows left occipital metastasis (*arrow*). Although enhancement is slightly less intense, mass is clearly visible and similar in size.

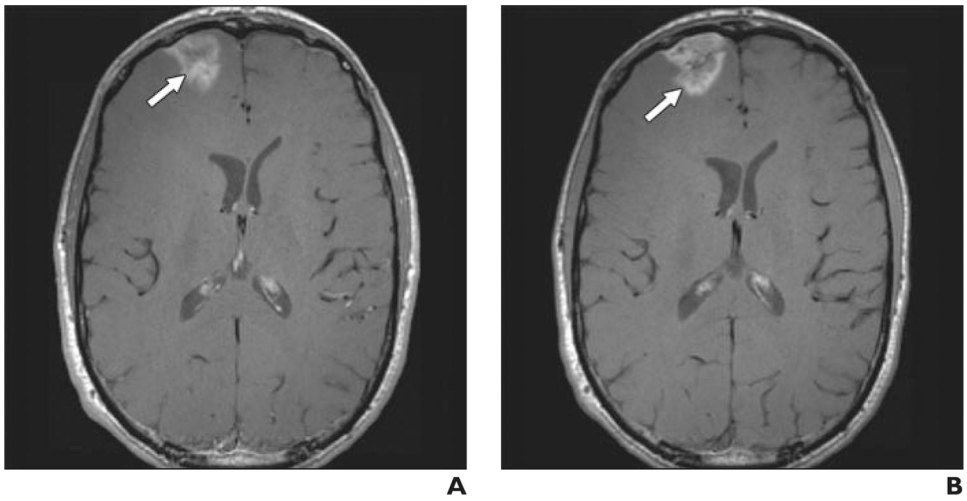

Fig. 3—.

34-year-old man with melanoma metastatic to brain.

A, Axial T1-weighted turbo spin-echo gadolinium-enhanced MR image, obtained according to protocol, shows right frontal lobe metastasis (*arrow*).

B, Axial T1 turbo spin-echo ferumoxytol-enhanced MR image obtained 2 days after image in **A** shows right frontal lobe metastasis (*arrow*).

TABLE 1:

Sequence Parameters for Imaging Protocol 813

Imaging Details	Sequence 1[a]	Sequence 2[b]	Sequence 3[c]	Sequence 4[d]
Unenhanced and gadolinium-enhanced MRI				
Contrast	Unenhanced	Unenhanced	Unenhanced	Contrast-enhanced
Image type	T1-weighted sagittal FFE	T1-weighted axial SE	T2-weighted axial TSE	T1-weighted MP-RAGE sagittal 3D TFE
FOV (mm)	180 × 240	180 × 240	180 × 240	230 × 230
Matrix	192 × 256	192 × 256	192 × 256	230 × 230
Slice thickness (mm)[e]	3	3	3	1
Ferumoxytol-enhanced MRI				
Image type	T1-weighted sagittal FFE	T1-weighted axial SE	T2-weighted axial TSE	T1-weighted MP-RAGE sagittal 3D TFE
FOV (mm)	180 × 240	180 × 240	180 × 240	230 × 230
Matrix	192 × 256	192 × 256	192 × 256	230 × 230
Slice thickness (mm)[e]	3	3	3	1

Note—For all study subjects, gadolinium-enhanced MRI examinations were performed immediately after administration of a standard 0.1 mmol/kg IV dose of gadoteridol. For ferumoxytol-enhanced MRI, baseline T1-weighted unenhanced imaging was performed on day 1 immediately before ferumoxytol injection. Ferumoxytol-enhanced MRI was performed 24 hours after IV injection of 510 mg of ferumoxytol diluted in normal saline to optimize anatomic enhancement detection (on day 2). FFE = fast-field echo, SE = spin echo, TSE = turbo spin echo, MP-RAGE = magnetization-prepared rapid acquisition gradient echo, TFE = turbo field echo.

[a]TR, 300 ms; number of signals acquired, 4.

[b]TR/TE, 700/14; number of signals acquired, 1.

[c]R/TE, 9000/72; number of signals acquired, 1.

[d]TR/TE, 8.2/3.8; number of signals acquired, 1; flip angle, 8°.

[e]All sections were contiguous and interleaved.

TABLE 2:

Sequence Parameters for Imaging Protocol 1562

Imaging Details	Sequence 1	Sequence 2	Sequence 3	Sequence 4
Unenhanced and gadolinium-enhanced MRI				
Image type	T1-weighted sagittal FFE[a]	T1-weighted axial SE[b]	T2-weighted axial TSE[c]	T1-weighted MP-RAGE sagittal 3D TFE[d]
FOV (mm)	180 × 240	180 × 240	180 × 240	230 × 230
Matrix	192 × 256	192 × 256	192 × 256	230 × 230
Slice thickness (mm)[e]	3	3	3	1
Gadolinium-enhanced MRI				
Image type	T1-weighted sagittal FFE[a]	T2-weighted axial TSE[c]	T1-weighted axial SE[b]	T1-weighted MP-RAGE sagittal 3D TFE[d]
FOV (mm)	180 × 240	180 × 240	180 × 240	230 × 230
Matrix	192 × 256	192 × 256	192 × 256	230 × 230
Slice thickness (mm)[e]	3	3	3	1
Ferumoxytol-enhanced MRI				
Image type	T1-weighted sagittal FFE[a]	T1-weighted axial SE[b]	T2-weighted axial TSE[c]	T1-weighted MP-RAGE sagittal 3D TFE[d]
FOV(mm)	180 × 240	180 × 240	180 × 240	230 × 230
Matrix	192 × 256	192 × 256	192 × 256	230 × 230
Slice thickness (mm)[e]	3	3	3	1

Note—For all study subjects, gadolinium-enhanced MRI examinations were performed immediately after administration of a standard 0.1 mmol/kg IV dose of gadoteridol. For ferumoxytol-enhanced MRI, baseline T1-weighted unenhanced imaging was performed on day 1 immediately before ferumoxytol injection. Ferumoxytol-enhanced MRI was performed 24 hours after IV injection of 510 mg of ferumoxytol diluted in normal saline to optimize anatomic enhancement detection (on day 2). FFE = fast-field echo, SE = spin echo, TSE = turbo spin echo, MP-RAGE = magnetization-prepared rapid acquisition gradient echo, TFE = turbo field echo.

[a]TR, 300 ms; number of signals acquired, 4.

[b]TR/TE, 700/14; number of signals acquired, 1.

[c]TR/TE, 9000/72; number of signals acquired, 1.

[d]TR/TE, 8.2/3.8; number of signals acquired, 1; flip angle, 8°.

[e]All sections were contiguous and interleaved.

TABLE 3:

Patient Demographics, Primary Cancer Diagnosis, and Number of Individual Metastatic Foci by Reviewer

Patient	Age (y)	Sex	Diagnosis	No. of Metastatic Foci on Gadolinium-Enhanced MRI		No. of Metastatic Foci on Ferumoxytol-Enhanced MRI		No. of New T2 Hypointense Lesions	
				Reviewer 1 (*n* = 72)	Reviewer 2 (*n* = 78)	Reviewer 1 (*n* = 77)	Reviewer 2 (*n* = 83)	Reviewer 1 (*n* = 54)	Reviewer 2 (*n* = 57)
1	70	Male	Melanoma	1	1	1	1	1	1
2	34	Male	Melanoma	1	1	1	1	1	1
3	56	Male	Lung cancer	1	1	1	1	1	1
4	48	Female	Breast cancer	12[a]	14[a]	11[a]	14[a]	6	6
5	39	Female	Breast cancer	8[a]	8[a]	7[a]	8[a]	3	4
6	54	Female	Uterine cancer	2	2	2	2	2	2
7	53	Male	Lung cancer	2	2	2	2	2	2
8	67	Male	Renal cell carcinoma	1	1	1	1	1	1
9	79	Male	Colon cancer	1	1	1	1	1	1
10	52	Female	Lung cancer	1	1	1	1	1	1
11	60	Male	Lung cancer	2	2	2	2	2	2
12	67	Female	Ovarian cancer	2[a]	3[a]	2[a]	3[a]	0	0
13	51	Female	Breast cancer	1	1	1	1	0	0
14	52	Female	Ovarian cancer	1	1	1	1	1	1
15	53	Male	Carcinoid tumor	3[a]	4[a]	3[a]	4[a]	3	3
16	50	Female	Melanoma	13	13	13	13	11	11
17	34	Female	Lung cancer	18[a]	20[a]	25[a]	25[a]	16	18
18	68	Female	Lung cancer	1	1	1	1	1	1
19	62	Male	Lung cancer	1	1	1	1	1	1

[a]Discrepancies were found between gadolinium-enhanced and ferumoxytol-enhanced MRI.